sustainability

MDPI

Article

Optimal Investments in PV Sources for Grid-Connected Distribution Networks: An Application of the Discrete–Continuous Genetic Algorithm

Oscar Danilo Montoya [1,2], Luis Fernando Grisales-Noreña [3] and Alberto-Jesus Perea-Moreno [4,*]

1 Facultad de Ingeniería, Universidad Distrital Francisco José de Caldas, Bogotá 110231, Colombia; odmontoyag@udistrital.edu.co
2 Laboratorio Inteligente de Energía, Universidad Tecnológica de Bolívar, Cartagena 131001, Colombia
3 Departamento de Electrómecanica y Mecatrónica, Instituto Tecnológico Metropolitano, Medellín 050028, Colombia; luisgrisales@itm.edu.co
4 Departamento de Física Aplicada, Radiología y Medicina Física, Campus de Rabanales, Universidad de Córdoba, 14071 Córdoba, Spain
* Correspondence: g12pemoa@uco.es

Abstract: The problem of the optimal siting and sizing of photovoltaic (PV) sources in grid connected distribution networks is addressed in this study with a master–slave optimization approach. In the master optimization stage, a discrete–continuous version of the Chu and Beasley genetic algorithm (DCCBGA) is employed, which defines the optimal locations and sizes for the PV sources. In the slave stage, the successive approximation method is used to evaluate the fitness function value for each individual provided by the master stage. The objective function simultaneously minimizes the energy purchasing costs in the substation bus, and the investment and operating costs for PV sources for a planning period of 20 years. The numerical results of the IEEE 33-bus and 69-bus systems demonstrate that with the proposed optimization methodology, it is possible to eliminate about 27% of the annual operation costs in both systems with optimal locations for the three PV sources. After 100 consecutive evaluations of the DCCBGA, it was observed that 44% of the solutions found by the IEEE 33-bus system were better than those found by the BONMIN solver in the General Algebraic Modeling System (GAMS optimization package). In the case of the IEEE 69-bus system, the DCCBGA ensured, with 55% probability, that solutions with better objective function values than the mean solution value of the GAMS were found. Power generation curves for the slack source confirmed that the optimal siting and sizing of PV sources create the duck curve for the power required to the main grid; in addition, the voltage profile curves for both systems show that voltage regulation was always maintained between ±10% in all the time periods under analysis. All the numerical validations were carried out in the MATLAB programming environment with the GAMS optimization package.

Keywords: distributed generation; PV sources; optimization algorithm; genetic algorithm; planing of electrical grids

Citation: Montoya, O.D.; Grisales-Noreña, L.F.; Perea-Moreno, A.-J. Optimal Investments in PV Sources for Grid-Connected Distribution Networks: An Application of the Discrete–Continuous Genetic Algorithm. *Sustainability* **2021**, *13*, 13633. https://doi.org/10.3390/su132413633

Academic Editor: Domenico Mazzeo

Received: 28 October 2021
Accepted: 6 December 2021
Published: 9 December 2021

1. Introduction

Electricity is a fundamental right worldwide, and all national governments and multiple independent organizations strive together to make this public service universally accessible [1,2]. However, this involves a colossal challenge: most countries use fossil fuels to generate electricity, which directly affects us, as the emission of environmental pollutants into the atmosphere leads to global warming [3,4]. Therefore, to extend electricity coverage and mitigate greenhouse gas emissions, most governments have created policies to motivate the electricity sector to invest in dispersed generation on a massive and integrated scale, mainly based on photovoltaic (PV) and wind technology [5–7]. In the Colombian context, in 2014, the Senate of the Republic approved the 1715 Law, which regulates the integration of dispersed generation into the electricity distribution sector [8,9]. This law has

significantly promoted the usage of renewable resources in urban and rural areas [10]; however, today, there exists in multiple regions of Colombia the unique possibility of generating electricity energy through diesel generators [11]. The most recent report (31 August 2021) of the Institute for Promoting Electricity Solutions in Non-Interconnected Areas (IPSE is the abbreviation for its Spanish name) shows the usage of diesel sources in Colombia compared with the incipient integration of renewable energies [12]. Currently, the total diesel generation capacity is about 267,911 kW, which benefits about 201,412 users, whereas for solar PV generation, the installed capacity is 21,710 kW, which benefits about 23,617 users. These values show that PV energy supplies less than 10% of the users that diesel sources do [12]. Figures 1 and 2 show the current state of the diesel and PV generation in Colombia.

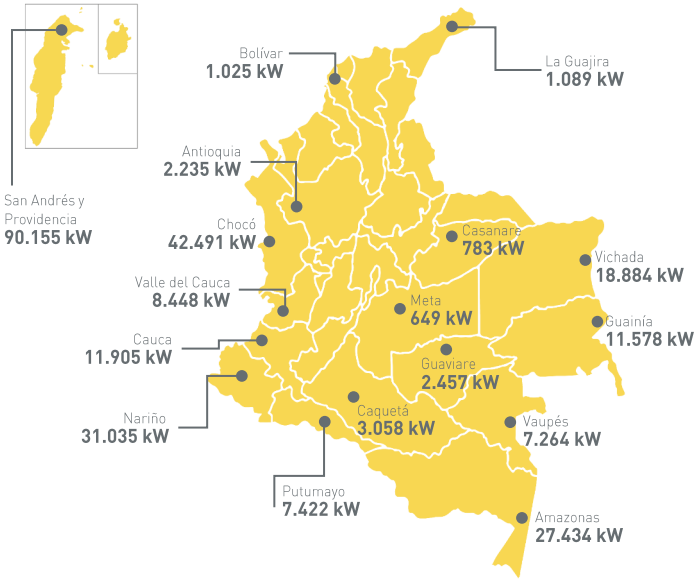

Figure 1. Installed diesel generation in Colombia (31 August 2021). Source: IPSE.

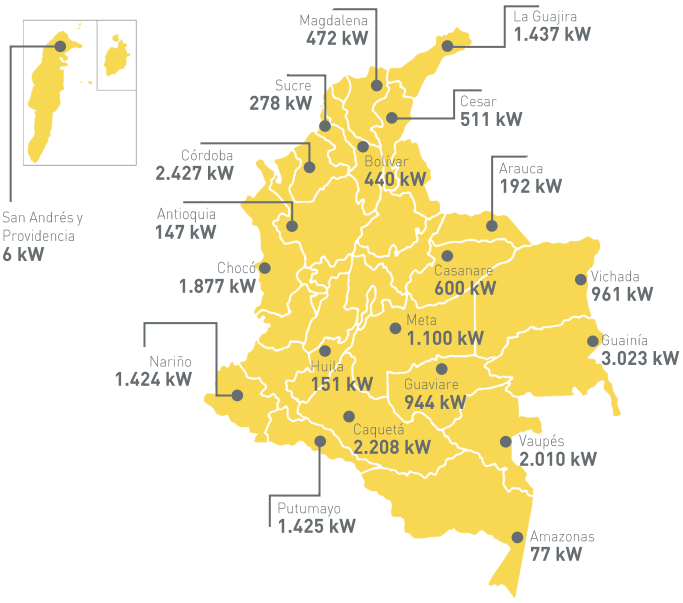

Figure 2. Installed PV generation in Colombia (31 August 2021). Source: IPSE.

The distributions of diesel generation and PV generation show that in Colombia, similarly to the cases of the Caribbean and Pacific regions, the potential of several solar resource-rich regions has not been realized [13]; however, this problem can be solved using sustainable energy solutions [11].

The possibility of integrating PV sources in countries such as Colombia is a certainty; nevertheless, after identifying promising areas where these solutions can provide clean energy to thousands of end-users [14], efficient optimization techniques that permit their optimal siting and sizing in the distribution network need to be proposed [15]. These solution strategies must consider economic and technical aspects. The economic considerations should include the generation costs of conventional sources and the investment and operating costs of PV sources [16]. The technical aspects should encompass voltage regulation and power balance equilibrium in all nodes of the network [17,18], among others.

To address the problem of the optimal placement and sizing of PV sources in electrical distribution networks, an objective function is proposed herein that involves the simultaneous minimization of the grid generation costs of conventional sources and the investment and operating costs of PV sources for a planning period of 20 years. The proposed optimization model is from the family of mixed-integer nonlinear programming (MINLP). For this reason, a discrete–continuous version of the Chu and Beasley genetic algorithm (DCCBGA), recently proposed in [19] to locate and size distribution static compensators, was employed in this study to solve the complete MINLP model.

In the literature, multiple optimization approaches can be found that aim to solve the problem of the optimal locations of dispersed generators in electrical distribution grids. Some of these approaches include particle swarm optimization [20], genetic algorithms [21], the sine–cosine algorithm [22], the population-based incremental learning optimizer [17], krill herd optimization [23], the vortex-search algorithm [15], and mathematical-based approaches in the General Algebraic Modeling System (GAMS) [24,25]. The main characteristic of these approaches is that the objective function considered is typically associated with the minimization of total grid losses in the peak hour condition, which is an unrealistic simulation case, owing to the fact that the loads and the renewables vary their behavior over the day [15].

Some of the literature has addressed the multi-period problem in distribution networks with renewable energies and batteries as follows: The authors of [16] proposed that battery energy storage systems and renewable generation in medium- and low-voltage distribution grids be optimally integrated. The problem was decoupled into two stages. A heuristic algorithm based on simulated annealing defined the locations of the distributed energy resources, and mixed-integer linear programming defined their optimal daily outputs. The numerical results of the test feeders composed of 11, 135, and 230 nodes demonstrated the efficiency of the proposed approach when compared with conic models. The authors of [26] studied the problem of the optimal siting and sizing of wind energy sources in distribution and transmission systems. They solved the exact MINLP model with the help of the GAMS optimization package. Their main contribution was the discovery of the reactive power capabilities of wind turbines to minimize grid energy losses. The main problem of the study is that the authors did not take into account costs in the objective function, which means that that the devices might have been over-sized. The same approach by the authors of [26] was extended in [27] to high-voltage transmissions networks while considering PV generators with dynamic active and reactive power capabilities. The exacted MINLP model was also solved in the GAMS environment; however, the investment and operating costs for renewables were not considered. Molina et al. in [28] proposed a convex optimization model based on second-order cone programming to minimize the total greenhouse gas emissions in distribution networks in rural areas by integrating PV sources. The proposed optimization approach ensures finding the global optimum; however, the authors did not include the economic aspects in the optimal sizing problem, which limits the applicability of their solution to real distribution grids.

With respect to the state-of-the-art research just mentioned, the main contributions of this study are the following:

- The formulation of an MINLP model that represents the problem of the optimal siting and sizing of PV sources in grid-connected distribution networks with the aim of

minimizing the total energy purchasing costs in the substation bus and the investment and operating costs of the PV sources for a planning horizon of 20 years.

- The solution of the MINLP model through an application of the DCCBGA, which has not been previously used for the studied problem. Numerical results demonstrated its superior performance when compared with the GAMS software in terms of response quality and convergence guarantee.

It is worth mentioning that the proposed study did not consider the presence of battery energy storage systems or controllable and referable loads, as we were interested in exploring solar solutions for grid-connected areas with minimum investment costs. However, the inclusion of these devices is an opportunity for future research [29,30]. Regarding the selection of the classical Chu and Beasley genetic algorithm (CBGA) and its discrete–continuous version of codification, which helps solve the problem of the optimal location and sizing of PV sources with a unified vector: it is important to say that this optimization algorithm was selected to solve the proposed MINLP model, as it is a widely known model and is used to solve complex optimization problems with efficient numerical performance and low computational effort. Moreover, the discrete–continuous version of the CBGA has recently yielded satisfactory results for the optimal reactive compensation problems, as reported in [19] for static compensators and in [31] for optimal reactive power flow in transmission systems.

The remainder of this research is organized as follows: Section 2 presents the general optimization model for the optimal location and sizing of PV sources in grid-connected distribution networks considering investment and operating costs for a planning period with N_t years. Section 3 presents the main aspects of the proposed optimization methodology, which is guided in the master stage by the DCCBGA, which uses the recursive solution of the power flow problem in the slave stage with the successive approximation power flow approach. Section 4 describes the main features of the IEEE 33-bus and IEEE 69-bus systems, including their load and branch parameters. It also presents the load generation and demand curves and the necessary parameters for evaluating the objective function. Section 5 presents the computational validation of the proposed methodology with the GAMS optimization package in both test feeders. Finally, Section 6 lists the main conclusions derived from this project and some recommendations for future studies.

2. Optimization Problem

The problem of the optimal siting and dimensioning of PV sources in distribution networks corresponds to an MINLP model that combines binary variables associated with the locations of the PV sources and continuous variables regarding power flows and current in branches and voltages in nodes, among others. The complete optimization model is presented below.

2.1. Objective Function

The rationale behind integrating PV sources with grid-connected distribution systems is to minimize the total energy purchasing costs in the substation bus that interfaces the distribution grid to the transmission/sub-transmission system. The objective function comprises the annualized costs of energy purchased at the substation bus and the annualized investment costs of PV sources, including their maintenance costs. The objective function is formulated as follows:

$$A_{\text{cost}} = f_1 + f_2, \tag{1}$$

$$f_1 = C_{\text{kWh}} T \left(\frac{t_a}{1-(1+t_a)^{-N_t}} \right) \left(\sum_{h\in\mathcal{H}} \sum_{i\in\mathcal{N}} p_{i,h}^{cg} \Delta h \right) \left(\sum_{t\in\mathcal{T}} \left(\frac{1+t_e}{1+t_a} \right)^t \right), \tag{2}$$

$$f_2 = C_{\text{PV}} \left(\frac{t_a}{1-(1+t_a)^{-N_t}} \right) \left(\sum_{i\in\mathcal{N}} p_i^{pv} \right) + C_{O\&M} T \sum_{i\in\mathcal{N}} \sum_{h\in\mathcal{H}} p_i^{pv} G_h^{pv} \Delta h, \tag{3}$$

where A_{cost} represents the total annual operative cost of the network; f_1 is the component of the objective function regarding the expected annualized energy purchasing costs in the substation buses; f_2 is the component of the objective function regarding the investment costs in PV sources and their maintenance and operation costs. C_{kWh} is the average energy purchasing costs in the substation bus; T represents the number of days in an ordinary year (i.e., 365 days); t_a corresponds to the internal return rate expected for investments made by the utility during the duration of the project; N_t is the total number of periods of the planning project in years; $p_{i,h}^{cg}$ is the active power generation output at each conventional generator connected at node i during the period of time h; Δh is the length of the time period where the electrical variables are assumed as constants; t_e is the average expected percentage of increment of the energy purchasing cost during the planing horizon. C_{PV} represents the average cost of installing a kW of PV power; p_i^{pv} is the size of a PV source connected at node i; $C_{O\&M}$ is the maintenance and operating costs of a PV source; G_h^{pv} is the expected PV generation curve in the area of influence of the distribution network. Note that $\mathcal{H}$, $\mathcal{N}$, and $\mathcal{T}$ are the sets that contain all the periods of time in a daily operation scenario, the nodes of the network, and the number of years of the planning period, respectively.

2.2. Set of Constraints

The set of constraints in the problem of the optimal placement and sizing of PV sources in grid-connected distribution networks includes active and reactive power balance constraints, voltage regulation bounds, and devices' capabilities, among other constraints. The complete list of constraints is listed below.

$$p_{i,h}^{cg} + p_i^{pv} G_h^{pv} - P_{i,h}^{d} = v_{i,h} \sum_{j \in \mathcal{N}} Y_{ij} v_{j,h} \cos\left(\theta_{i,h} - \theta_{j,h} - \varphi_{ij}\right), \ \{\forall i \in \mathcal{N}, \ \forall h \in \mathcal{H}\}, \tag{4}$$

$$q_{i,h}^{cg} - Q_{i,h}^{d} = v_{i,h} \sum_{j \in \mathcal{N}} Y_{ij} v_{j,h} \sin\left(\theta_{i,h} - \theta_{j,h} - \varphi_{ij}\right), \ \{\forall i \in \mathcal{N}, \ \forall h \in \mathcal{H}\}, \tag{5}$$

$$p_i^{cg,\min} \leq p_{i,h}^{cg} \leq p_i^{cg,\max}, \ \{\forall i \in \mathcal{N}, \ \forall h \in \mathcal{H}\} \tag{6}$$

$$q_i^{cg,\min} \leq q_{i,h}^{cg} \leq q_i^{cg,\max}, \ \{\forall i \in \mathcal{N}, \ \forall h \in \mathcal{H}\} \tag{7}$$

$$x_i p_i^{pv,\min} \leq p_i^{pv} \leq x_i p_i^{pv,\max}, \ \{\forall i \in \mathcal{N}\}, \tag{8}$$

$$v_i^{\min} \leq v_{i,h} \leq v_i^{\max}, \ \{\forall i \in \mathcal{N}, \ \forall h \in \mathcal{H}\} \tag{9}$$

$$\sum_{i \in \mathcal{N}} x_i \leq N_{pv}^{ava}, \tag{10}$$

$$x_i \in \{0, 1\}, \ \{\forall i \in \mathcal{N}\}, \tag{11}$$

where $P_{i,h}^{d}$ and $Q_{i,h}^{d}$ are the active and reactive power demands at node i over the period of time h; $q_{i,h}^{cg}$ is the reactive power injection in the conventional source connected at node i during the period of time h; $v_{i,h}$ and $v_{j,h}$ are the voltage magnitudes at nodes i and j, respectively, during the period of time h; Y_{ij} is the magnitude of the admittance that relates nodes i and j, which has an angle φ_{ij}; $\theta_{i,h}$ and $\theta_{j,h}$ are the voltage angle values in nodes i and j at each period of time; $p_i^{cg,\min}$ and $p_i^{cg,\max}$ are the active generation bounds associated with the conventional generator connected at node i, and $q_i^{cg,\min}$ and $q_i^{cg,\max}$, respectively, are its corresponding reactive power generation bounds. x_i is the binary variable associated with the installation ($x_i = 1$) or not ($x_i = 0$) of a PV source at node i; $p_i^{pv,\min}$ and $p_i^{pv,\max}$ are the minimum and maximum sizes allowed for the PV integration in the distribution grid, respectively. $v_i^{\min}$ and $v_i^{\max}$ represent the minimum and maximum voltage regulation bounds allowed at node i; N_{pv}^{ava} is a constant parameter associated with the maximum number of PV sources available for installation along with the distribution grid.

2.3. Model Interpretation

The interpretation of the MINLP model defined from (1) to (11) is the following: Equation (1) defines the objective function of the optimization problem, which adds the energy purchasing costs in the conventional generators (i.e., substation buses) as defined in Equation (2) and the annualized investments in PV sources, including its maintenance and operating costs as defined by Equation (3). The equality constraints (4) and (5) present the active and reactive power equilibria at each node of the system for each period of time. These equations are the most complex constraints in the studied problem, as these are nonlinear non-convex and typically require numerical methods to be addressed properly. Box-type constraints (6) and (7) define the lower and upper bounds associated with the active and reactive power generation outputs in the conventional sources; box-type constraint (9) defines the PV lower and upper generation capabilities for the PV sources in the case that the binary variable gets activated; box-type constraint (10) presents the lower and upper voltage regulation limits allowed for all nodes of the network. This is a typical constraint imposed by regulatory entities and utility operation practices. The inequality constraint (10) limits the maximum number of PV sources that can be installed along with the distribution network; finally, constraint (11) shows the binary nature of the decision variable regarding the location or not of a PV source in a particular node of the network.

To characterize the optimization model (1)–(11) in Table 1, the following have been presented: the number of variables of the optimization problem, their nature, and the number and types of constraints. Note that n (number of nodes) is defined as the cardinality of the set $\mathcal{N}$, and p (number of periods of time) the cardinality of the set $\mathcal{H}$.

Table 1. Numbers of variables and constraints in the optimization model (1)–(11).

Variables	**Type**	**Number**
PV locations	Binary	n
Active powers	Real	$2np$
Reactive powers	Real	np
Voltage magnitudes	Real	np
Voltage angles	Real	np
Objective function	Real	3
Total variables	Real + Binary	$n(5p+1)+3$
Constraints	**Type**	**Number**
Active power balance	Equality	np
Reactive power balance	Equality	np
Conventional generation bounds	Inequality (box-type constraint)	$2np$
PV sizes	Inequality (box-type constraint)	n
Voltage regulation	Inequality (box-type constraint)	np
Number of PV sources	Inequality	1
Objective function	Equality	3
Total constraints	Equalities + Inequalities	$n(5p+1)+4$

It is worth mentioning that the main complication of the optimization model (1)–(11) is its MINLP nature, as it combines binary and continuous variables with nonlinear non-convex relations mainly defined by the power balance equations. To solve this kind of problem, the use of master–slave optimization methodologies is recommended. These allow the decoupling of the location problem from the sizing problem [32]. In the following section, a master–slave optimization methodology is presented, which allows the MINLP model to be solved (1)–(11) by combining the DCCBGA with the successive approximation power flow method.

3. Proposed Solution Methodology

To deal with the problem of the optimal placement and sizing of PV sources in grid-connected distribution grids, in this study, we propose the application of the DCCBGA [33]. The main advantage of this approach is that the proposed codification defines the optimal locations and sizes of the PV sources in a unique vector, which reduces one stage in the classical optimization methods, where an additional optimization algorithm is used to define their sizes [34].

The proposed codification has the following structure:

$$\left[2,\ k\ ,\ldots,\ n \mid p_2^{pv},\ p_k^{pv}\ ,\ldots,\ p_n^{pv}\right], \tag{12}$$

where its dimensionality is $1 \times 2N_{pv}^{ava}$. The first N_{pv}^{ava} is associated with the nodes where the PV sources will be installed (discrete part of the codification), and the second relates to their optimal sizes (continuous part of the codification). Note that with the usage of this codification, the proposed optimization methodology is composed of two stages, which are the master stage guided by the CBGA, and the slave optimization stage, where a power flow is used to evaluate the first component of the objective function, i.e., the total energy purchasing costs in the conventional sources. The main characteristics of the master and slave optimization stages are illustrated in Figure 3.

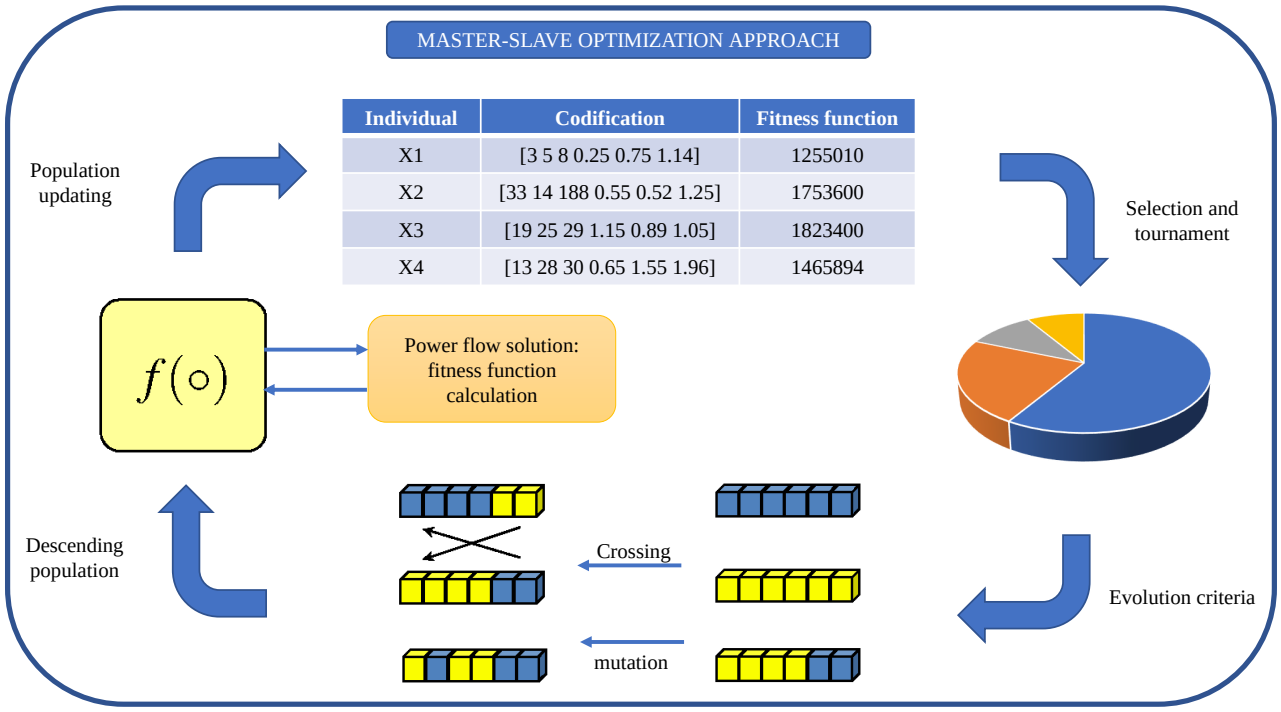

Figure 3. Integration of a master–slave optimization approach to solving combinatorial problems.

As previously mentioned, the master stages are entrusted with guiding the exploration and exploitation of the solution space through the application of the evolution criteria to an initial population; however, to know the value of the fitness function (objective function plus penalizations), the use of a slave stage entrusted with solving the multiperiod power flow problem is required. Each stage is presented in detail below.

3.1. Master Optimization Stage

The master optimization stage can be defined as the brain of the solution methodology, as this is entrusted with defining the best set of candidate solutions with the structure presented in (12). This is done by applying different evolution criteria, which, in turn, is done by initializing these solutions with a random procedure that ensures their optimal

dispersion in the solution space. In the flowchart presented in Figure 4, the main aspects of the proposed DCCBGA to define the optimal placement and sizing of PV sources in grid-connected distribution systems are summarized.

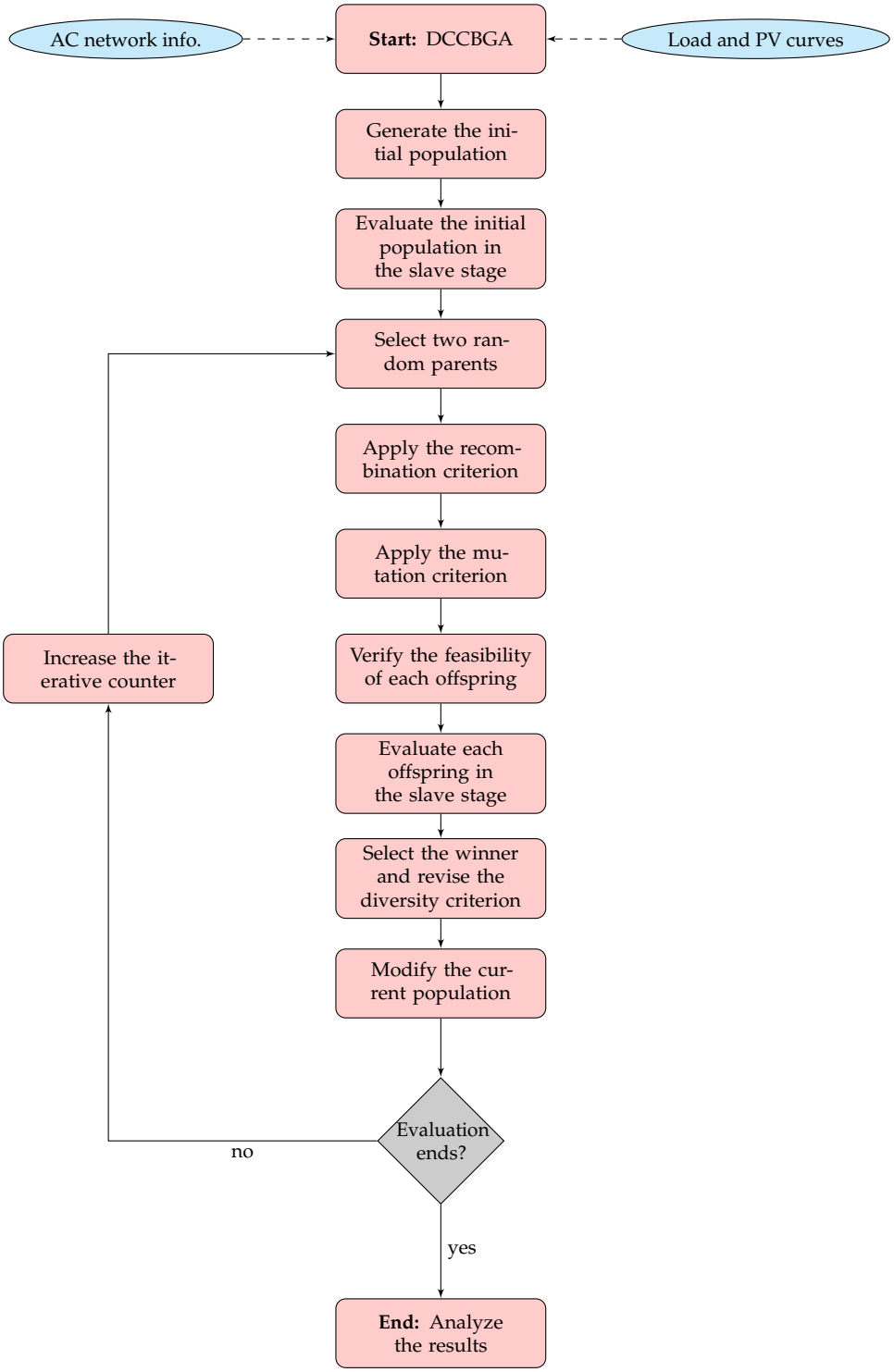

Figure 4. General implementation of the proposed DCCBGA for solving any optimization problem.

From Figure 4, which describes the general implementation of the proposed DCCBGA, we can note the following:

- ✓ The initial population is generated randomly in the solution space using a Gaussian distribution with normal form. This initial population corresponds to a matrix with n_i rows, each of them with the structure presented in Equation (12).
- ✓ The slave stage is the heart of the optimization methodology, as it allows the fitness function of the initial population and the offspring population to be known. This stage is presented in detail in the following section.
- ✓ The tournament is avoided by directly selecting two parents from the population. In addition, the recombination and the mutation criteria are applied for both offspring with 100% probability.
- ✓ Both mutated offspring are evaluated in the slave stage, and the best individual (lower fitness function value) is selected with the opportunity to become part of the current population if the diversity criterion is fulfilled and its fitness function is at least better than the worst parent in the population.

For additional details regarding the implementation of the CBGA in optimization, refer to the references [33,34].

3.2. Slave Stage: Power Flow Solution

The slave stage, as previously mentioned, corresponds to the heart (core) of the optimization strategies based on metaheuristics, as this allows the exploration and exploitation of the solution space to be guided [34]. In the case of the optimal siting and sizing of PV sources in the solution space, the slave stage is defined by the recursive evaluation of the power flow problem [17]. Here, we adopt the successive approximations power flow method initially proposed by Montoya and Gil-González in [35]. The main advantage of this power flow approach is that its numerical convergence can be ensured through the application of the Banach fixed-point theorem [36].

The general recursive power flow formula based on the successive approximation power flow method takes the following form:

$$\mathbb{V}_{d,h}^{m+1} = \mathbb{Y}_{dd}^{-1}\left[\mathbf{diag}^{-1}\left(\mathbb{V}_{d,h}^{\star,t}\right)\left(\mathbb{S}_{pv,h}^{\star} - \mathbb{S}_{d,h}^{\star}\right) - \mathbb{Y}_{ds}\mathbb{V}_{s,h}\right], \tag{13}$$

where m is the iterative counter; $\mathbb{V}_{d,h}$ is a complex vector that contains all the voltage variables in the demand nodes (for $m = 0$, it is assumed that $\mathbb{V}_{d,h}^{m+1} = 1\angle 0°$); $\mathbb{Y}_{dd}$ and $\mathbb{Y}_{ds}$ are admittance matrices that relate demand and slack nodes among them; $\mathbb{S}_{pv,h}^{\star}$ is a complex vector that contains all the power injections in the PV sources; $\mathbb{S}_{d,h}$ is a complex vector that contains all the constant power consumptions in the demand nodes; $\mathbb{V}_{s,h}$ represents the complex voltage outputs in the slack nodes (this value is perfectly known for power flow studies). Note that operator $\mathbf{diag}(Z)$ becomes the vector Z in a diagonal matrix; $Z^{\star}$ represents the complex conjugate value of the vector Z.

Note that the evaluation of the recursive formula (13) is made until the difference between both consecutive voltages fulfills the convergence criterion, i.e.,

$$\max\left\{\left|\left|\mathbb{V}_{d,h}^{m+1}\right| - \left|\mathbb{V}_{d,h}^{m}\right|\right|\right\} \leq \epsilon, \tag{14}$$

where ϵ is the convergence error, which, as recommended in [35], is assigned as 1×10^{-10}.

It is worth mentioning that the master stage for each solution individual in the current population sends the values of the $\mathbb{S}_{pv}^{\star}$ to evaluate the power flow problem and determine its corresponding fitness function value.

In the case of the calculation of the active power injections in the slack node, once the power flow problem is evaluated for each period of time, then, the complex power injection in the slack source (i.e., $\mathbb{S}_{cg,h}$) is calculated as follows:

$$\mathbb{S}_{cg,h}^{\star} = \mathbf{diag}\left(\mathbb{V}_{s,h}^{\star}\right)\left[\mathbb{Y}_{sd}\mathbb{V}_{d,h} + \mathbb{Y}_{ss}\mathbb{V}_{s,h}\right]. \tag{15}$$

Once the power flow problem is solved for each period of time as defined in (13) and the complex power generation in the slack node is calculated, the fitness function is assigned for each individual. The fitness function helps with the evolution of the optimization algorithm to find the minimum value of the objective function that is always feasible. The fitness function (F_f) in this study takes the following form:

$$F_f = A_{\text{cost}} + \alpha_1 \max_h \{0, |\mathbb{V}_{d,h}| - v_{\max}\} - \alpha_2 \min_h \{0, |\mathbb{V}_{d,h}| - v_{\min}\}, \quad (16)$$

where α_1 and α_2 are the penalization factors associated with the violation of the voltage regulation bounds, which generates an adaptive penalization as a function of the deviation value regarding the lower and upper voltage bounds. Note that the fitness function is equal to the objective function when all the constraints in the mathematical model (1)–(11) are fulfilled.

It is worth mentioning that the maximum and minimum power generation bounds of the PV sources are always ensured with the proposed codification of the DCCBGA, and the active and reactive power generation bounds in the slack source are not considered, as these are assumed to have enough capabilities to support all demands even if no PV sources are located on the grid.

4. Test Feeders

To validate the effectiveness and robustness of the proposed optimization approach to define the optimal locations and sizing of PV sources in grid-connected distribution networks, two classical test feeders composed of 33 and 69 nodes were used. These test feeders are depicted in Figure 5.

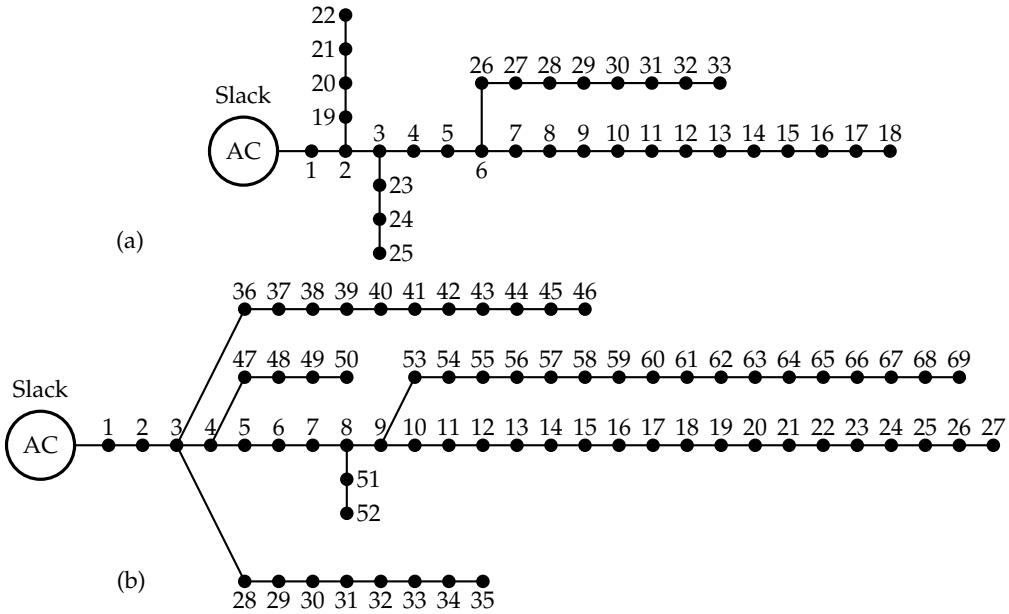

Figure 5. Distribution grids under analysis: (**a**) IEEE 33-bus system and (**b**) IEEE 69-bus system.

The main characteristic of these electrical networks is that they operate at the substation bus with an output voltage of 12.66 kV. The electrical parameters for these grids are reported in Tables 2 and 3, respectively.

Table 2. Branch and load parameters of the IEEE 33-bus system.

Node i	Node j	R_{ij} (Ω)	X_{ij} (Ω)	P_j (kW)	Q_j (kvar)	Node i	Node j	R_{ij} (Ω)	X_{ij} (Ω)	P_j (kW)	Q_j (kvar)
1	2	0.0922	0.0477	100	60	17	18	0.7320	0.5740	90	40
2	3	0.4930	0.2511	90	40	2	19	0.1640	0.1565	90	40
3	4	0.3660	0.1864	120	80	19	20	1.5042	1.3554	90	40
4	5	0.3811	0.1941	60	30	20	21	0.4095	0.4784	90	40
5	6	0.8190	0.7070	60	20	21	22	0.7089	0.9373	90	40
6	7	0.1872	0.6188	200	100	3	23	0.4512	0.3083	90	50
7	8	1.7114	1.2351	200	100	23	24	0.8980	0.7091	420	200
8	9	1.0300	0.7400	60	20	24	25	0.8960	0.7011	420	200
9	10	1.0400	0.7400	60	20	6	26	0.2030	0.1034	60	25
10	11	0.1966	0.0650	45	30	26	27	0.2842	0.1447	60	25
11	12	0.3744	0.1238	60	35	27	28	1.0590	0.9337	60	20
12	13	1.4680	1.1550	60	35	28	29	0.8042	0.7006	120	70
13	14	0.5416	0.7129	120	80	29	30	0.5075	0.2585	200	600
14	15	0.5910	0.5260	60	10	30	31	0.9744	0.9630	150	70
15	16	0.7463	0.5450	60	20	31	32	0.3105	0.3619	210	100
16	17	1.2890	1.7210	60	20	32	33	0.3410	0.5302	60	40

Table 3. Branch and load parameters of the IEEE 69-bus system.

Node i	Node j	R_{ij} (Ω)	X_{ij} (Ω)	P_j (kW)	Q_j (kvar)	Node i	Node j	R_{ij} (Ω)	X_{ij} (Ω)	P_j (kW)	Q_j (kvar)
1	2	0.0005	0.0012	0	0	3	36	0.0044	0.0108	26	18.55
2	3	0.0005	0.0012	0	0	36	37	0.0640	0.1565	26	18.55
3	4	0.0015	0.0036	0	0	37	38	0.1053	0.1230	0	0
4	5	0.0251	0.0294	0	0	38	39	0.0304	0.0355	24	17
5	6	0.3660	0.1864	2.6	2.2	39	40	0.0018	0.0021	24	17
6	7	0.3810	0.1941	40.4	30	40	41	0.7283	0.8509	1.2	1
7	8	0.0922	0.0470	75	54	41	42	0.3100	0.3623	0	0
8	9	0.0493	0.0251	30	22	42	43	0.0410	0.0475	6	4.3
9	10	0.8190	0.2707	28	19	43	44	0.0092	0.0116	0	0
10	11	0.1872	0.0619	145	104	44	45	0.1089	0.1373	39.22	26.3
11	12	0.7114	0.2351	145	104	45	46	0.0009	0.0012	39.22	26.3
12	13	1.0300	0.3400	8	5	4	47	0.0034	0.0084	0	0
13	14	1.0440	0.3450	8	5.5	47	48	0.0851	0.2083	79	56.4
14	15	1.0580	0.3496	0	0	48	49	0.2898	0.7091	384.7	274.5
15	16	0.1966	0.0650	45.5	30	49	50	0.0822	0.2011	384.7	274.5
16	17	0.3744	0.1238	60	35	8	51	0.0928	0.0473	40.5	28.3
17	18	0.0047	0.0016	60	35	51	52	0.3319	0.1114	3.6	2.7
18	19	0.3276	0.1083	0	0	9	53	0.1740	0.0886	4.35	3.5
19	20	0.2106	0.0690	1	0.6	53	54	0.2030	0.1034	26.4	19
20	21	0.3416	0.1129	114	81	54	55	0.2842	0.1447	24	17.2
21	22	0.0140	0.0046	5	3.5	55	56	0.2813	0.1433	0	0
22	23	0.1591	0.0526	0	0	56	57	1.5900	0.5337	0	0
23	24	0.3460	0.1145	28	20	57	58	0.7837	0.2630	0	0
24	25	0.7488	0.2475	0	0	58	59	0.3042	0.1006	100	72
25	26	0.3089	0.1021	14	10	59	60	0.3861	0.1172	0	0
26	27	0.1732	0.0572	14	10	60	61	0.5075	0.2585	1244	888
3	28	0.0044	0.0108	26	18.6	61	62	0.0974	0.0496	32	23
28	29	0.0640	0.1565	26	18.6	62	63	0.1450	0.0738	0	0
29	30	0.3978	0.1315	0	0	63	64	0.7105	0.3619	227	162
30	31	0.0702	0.0232	0	0	64	65	1.0410	0.5302	59	42
31	32	0.3510	0.1160	0	0	11	66	0.2012	0.0611	18	13
32	33	0.8390	0.2816	14	10	66	67	0.0047	0.0014	18	13
33	34	1.7080	0.5646	19.5	14	12	68	0.7394	0.2444	28	20
34	35	1.4740	0.4873	6	4	68	69	0.0047	0.0016	28	20

To evaluate the daily performance of the PV generation, we employed typical Colombian generation and demand curves, as presented in Figure 8 [37].

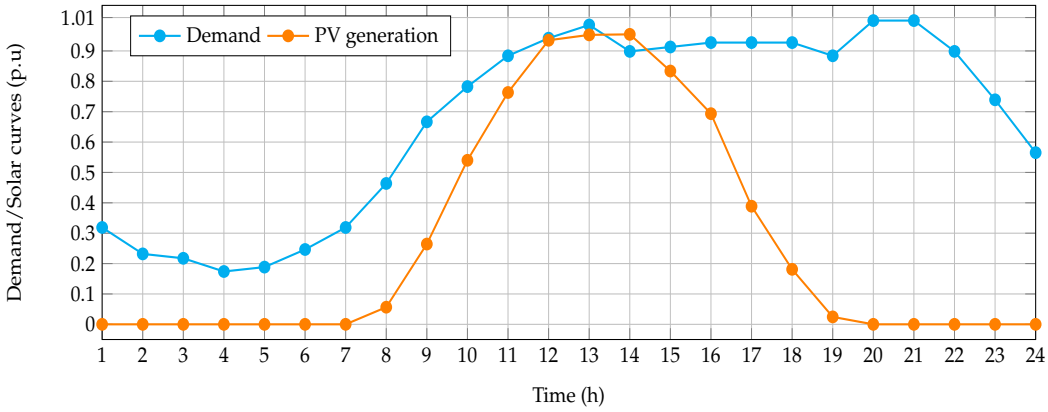

Figure 6. Typical behavior of the constant power consumption and the solar generation.

To determine the objective function value, the parameters reported in Table 4 are considered. Note that some of these parameters were taken from [19,38].

Table 4. Parameters used in the objective function calculation.

Parameter	Value	Unit	Parameter	Value	Unit
C_{kWh}	0.1390	US$/kWh	T	365	days
t_a	10	%	t_e	2	%
N_t	20	years	Δh	1	h
C_{PV}	1036.49	US$/kWp	$C_{O\&M}$	0.0019	US$/kWh
$p_i^{pv,\max}$	2400	kW	$p_i^{pv,\min}$	0	kW
N_{pv}^{ava}	3	—	ΔV	± 10	%
α_1	100×10^3	US$/V	α_2	100×10^3	US$/V

Regarding the parametrization of the proposed DCCBGA, we considered a population size composed of 10 individuals, 1000 iterations, and 100 consecutive repetitions; in the case of the power flow, a convergence error $\epsilon = 1 \times 10^{-10}$ and 100 iterations were considered as parameters.

5. Numerical Validation

The solution of the MINLP model defined from (1)–(11) was implemented in the GAMS software with the solvers BONMIN and COUENNE and with the MATLAB programming environment using its own scripts. In the case of the MATLAB implementations, its 2021*b* version was used on a PC with an AMD Ryzen 7 3700 2.3 GHz processor and 16.0 GB RAM, running on a 64 bit version of Microsoft Windows 10 Single Language.

To verify that the GAMS and MATLAB models are completely equivalent, we evaluated the benchmark case for both test feeders in both programming environments. All the numerical results for the these test feeders are reported below.

5.1. Results for the IEEE 33-Bus System

Table 5 presents the numerical results of the proposed DCCBGA and the GAMS solvers and the benchmark case. Note that the COUENNE solver diverged after 3600.37 s of exploration of the solution space. In the case of the BONMIN solver, it reached the solution in 3.64 s, whereas the proposed DCCBGA took about 5.30 s to solve the MINLP model (1)–(11).

Table 5. Numerical results for the IEEE 33-bus system for the proposed and GAMS solvers.

Method	Site (Node)	Size (kW)	A^{cost} (US$/year)	f_1 (US$/year)	f_2 (US$/year)
Bench. case	—	—	3,700,455.38	3,700,455.38	0
BONMIN	{17, 18, 33}	{1353.93, 210.51, 2145.15}	2,701,824.14	2,233,247.50	468,576.64
DCCBGA	{11, 15, 30}	{760.46, 968.97, 1905.98}	2,699,932.29	2,240,724.98	459,207.31

The numerical results in Table 5 show the following: (i) The BONMIN solver in GAMS got stuck in a local optimal solution where nodes 17, 18, and 33 were selected as the best optimal positions with a total installed power capacity of 3709.59 kWp. (ii) The solution of the DCCBGA is a better optimal solution with an additional improvement of the objective function by about US$1891.85 per year of operation with respect to the BONMIN solution. The optimal locations identified by the DCCBGA correspond to the nodes 11, 15, and 30, with a total installed power capacity of 3635.42 kWp. Note that the DCCBGA solution installs 74.17 kWp of generation less than the BONMIN solution, which reduces the annualized investment and energy purchasing cost by about US$7477.48 with respect to the BONMIN solution. (iii) In terms of percentages, the BONMIN solution allows a reduction in the annual grid costs by about 26.99% (i.e., about US$998,631.24), whereas the improvement of the proposed DCCBGA is 27.04%, i.e., US$1,000,523.09 per year of operation.

To validate the effectiveness and robustness of the DCCBGA for the studied problem, 100 consecutive evaluations of the the methodology were performed. These evaluations yielded the following results: a minimum objective function value of US$/year 2,699,932.29, a mean value of US$/year 2,702,178.35, and a maximum value of US$/year 2,705,870.99. Note that the standard deviation obtained by our proposal was 1221.67 dollars, which means that all the solutions were mainly concentrated in a ball with a small radius with respect to the mean value. The efficiency of the proposed DCCBGA for solving the MINLP model (1)–(11) is depicted in Figure 7; the solutions were normalized by the optimal solution obtained by the BONMIN solver. This graphic shows that 44 solutions with better numerical performance than the BONMIN solver were produced, which means that the proposed DCCBGA ensures, with 44% probability, the finding of a better solution when compared with the BONMIN solution in the IEEE 33-bus system.

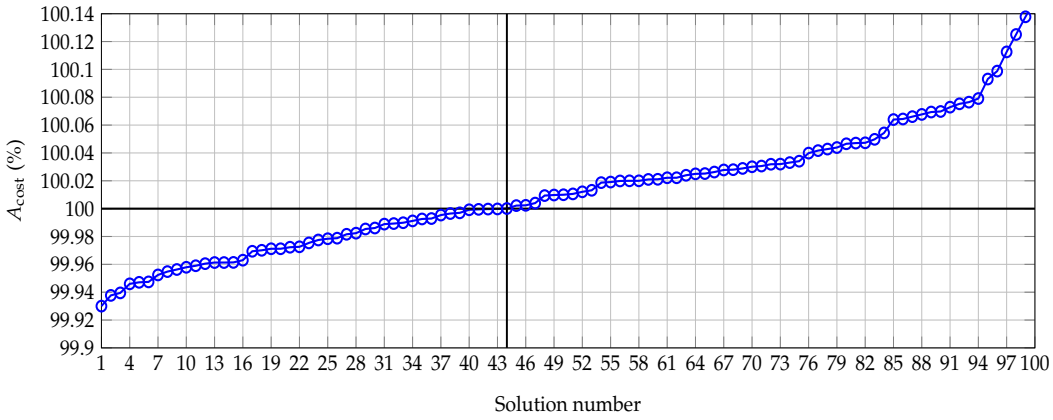

Figure 7. Percentage of efficiency of the DCCBGA with respect to the BONMIN solution.

To illustrate the effect of the PV generation in the generation output on the slack bus, Figure 7 compares the power generation in the slack node in the benchmark case with the values provided by the DCCBGA and BONMIN solvers.

The behavior of the power output in the slack source depicted in Figure 8 shows, as expected, that in the benchmark case, the total generation in the slack source followed the aggregated demand curve in the substation terminals. However, when PV sources were installed with the proposed DCCBGA and/or using the BONMIN solution, the well-known

duck curve was obtained, which allows the slack generation to be minimized in the time periods where enough PV energy is available [39].

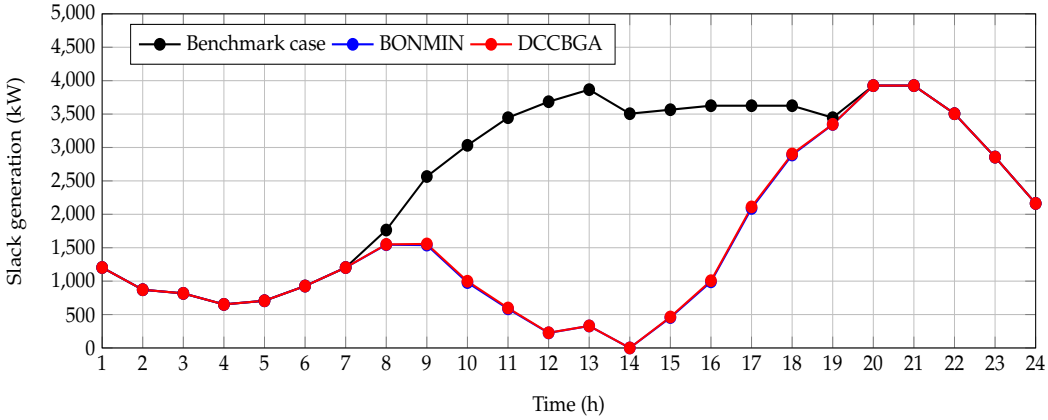

Figure 8. Behavior of the power generation in the slack source with and without optimal injection in PV sources in the IEEE 33-bus system.

To verify that the fitness function proposed ensures that the voltage profiles are within ±10% of the optimum, Figure 9 reports the minimum and maximum voltages obtained at each period of time.

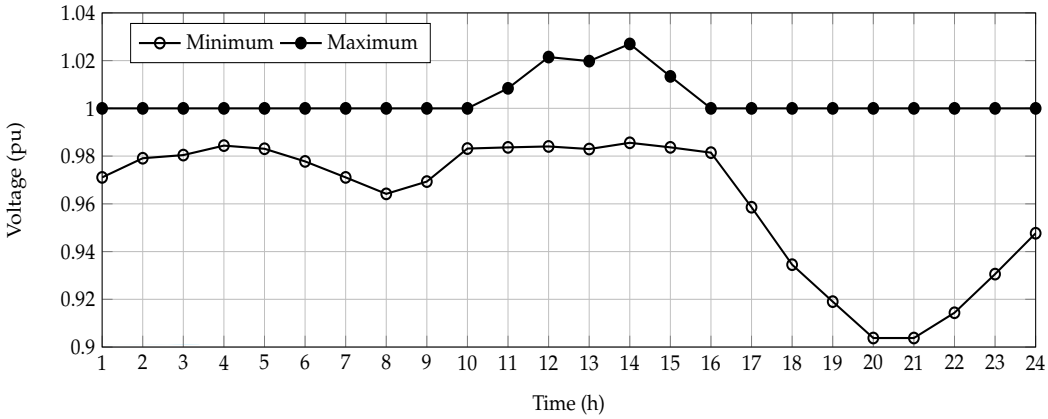

Figure 9. Minimum and maximum voltage magnitudes in the IEEE 33-bus system when the DCCBGA solution was implemented.

From Figure 9 it is possible to note that for all periods of time, the voltage profile of the network fulfills the imposed upper and lower regulation bounds (all the voltage magnitudes must be contained between the upper and lower curves presented in Figure 9). In addition, when the amount of PV power injection is significant, there are some periods where few nodes have voltage magnitudes more than the slack source with a maximum value of 1.0215 pu, and the minimum voltage value is as expected when the active and reactive power demand is maximum and the PV power injection is zero, i.e., in the time period 20 with a value of 0.90378 pu.

5.2. Results for the IEEE 69-Bus System

Table 6 presents the numerical results of the proposed DCCBGA for the IEEE 69-bus system. It is worth mentioning that both GAMS solvers diverged after more than one hour of solution space exploration, whereas the proposed DCCBGA took about 22.36 s to solve the MINLP model (1)–(11).

Table 6. Numerical results for the IEEE 69-bus system for the proposed DCBGA.

Method	Site (Node)	Size (kW)	A^{cost} (US$/year)	f_1 (US$/year)	f_2 (US$/year)
Bench. case	—	—	3,878,199.93	3,878,199.93	0
DCCBGA	{24, 61, 64}	{532.55, 1895.42, 1377.16}	2,825,783.32	2,345,138.38	480,644.95

Note that the optimal sites to assign PV sources in the IEEE 69-bus system, as presented in Table 6, are the nodes 24, 61, and 64 with a total installed power capacity of 3805.13 kWp. These power injections in the nominal operative conditions allow the total grid operative costs to be reduced by about 27.14% with respect to the benchmark case.

It is worth mentioning that after 100 consecutive evaluations of the proposed DCCBGA, the following values were obtained: a minimum value of US$/year 2,825,783.32, a maximum value of US$/year 2,844,469.50, a mean value of US$/year 2,829,498.36, and a standard deviation of US$/year 2827.18. These values imply the following: (i) All the solutions are near to the mean value, concentrated inside of a ball with a radius less than 3000 dollars. (ii) The minimum annual reduction in the operation costs is 26.65% for the maximum solution provided by the DCCBGA. (iii) The difference between the extreme solutions obtained by the DCCBGA is US$/year 18,686.18, i.e., less than 0.48% of the total annual operative costs in the benchmark case.

Figure 10 shows the percentage of efficiency reached by the DCCBGa when all the solutions were normalized to the mean value. This plot allows one to observe that there exist 55 solutions that ensure values lower than the mean value, i.e., annual operating costs of US$/year 2,829,498.36, which implies that the proposed method ensures, with 55% probability, a reduction of 27.04% with respect to the benchmark case.

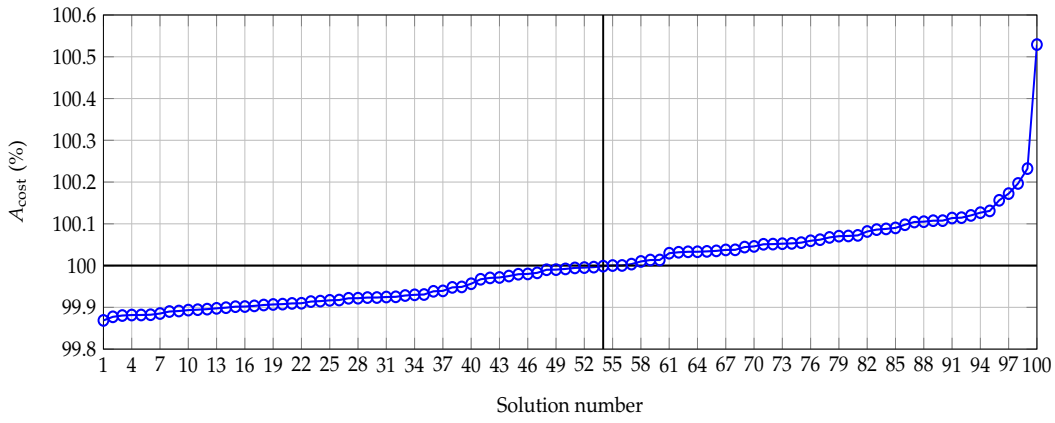

Figure 10. Percentage of efficiency of the DCCBGA with respect to the mean value in the IEEE 69-bus system.

It is worth mentioning that solutions 99 and 100 can be considered spurious solutions, as these are far from the mean values. However, both solutions ensured more than 26.65% improvements when compared with the benchmark case.

Figure 11 presents the daily generation behavior in the slack source in the benchmark case and for the optimal solution provided by the DCCBGA. Note that similarly to the IEEE 33-bus system, when PV sources were integrated, the slack generation fit a duck curve, in which a period (time 14) exists where the slack generation is only 2.4854 kW. This implies most of the demand is merely supported by PV generation.

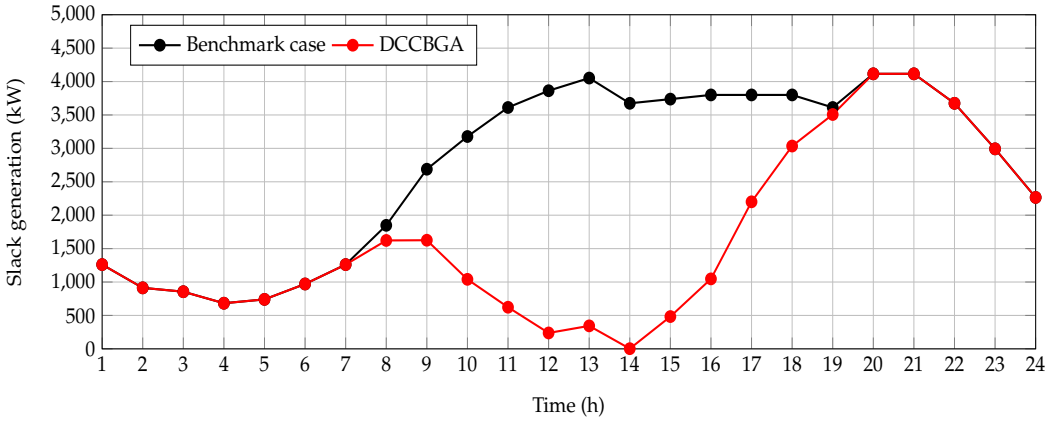

Figure 11. Behavior of the power generation in the slack source with and without optimal injection in PV sources in the IEEE 69-bus system.

Finally, Figure 12 shows that all the voltage profiles in all the nodes of the network fulfill the ±10% of maximum deviation with respect to the nominal substation voltage. Note that when the generation from PV sources is maximum, the voltage profile is greater than the substation value with a magnitude of 1.0388 pu. In addition, when the demand is maximum and the PV power injection is zero, the minimum voltage magnitude is 0.90919 pu. These extreme values confirm that the voltage regulation constraint was fulfilled in all the periods of time.

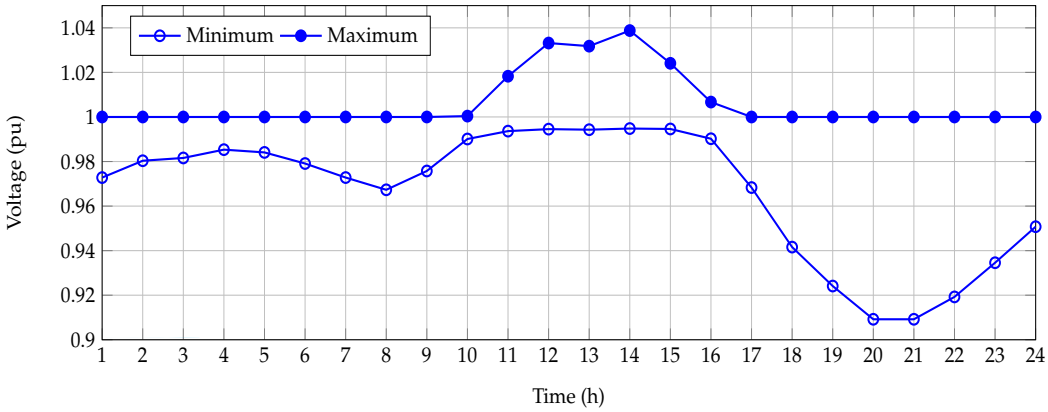

Figure 12. Minimum and maximum voltage magnitudes in the IEEE 69-bus system when the DCCBGA solution was implemented.

5.3. Complementary Results

To observe the effect of the power generation availability of the PV sources on the total operative costs of the network, we evaluated the variations in the PV generation from 50% to 100% in steps of 10%. The effect of these variations is observed in Table 7, where the total net savings are listed for both test feeders.

The numerical results in Table 7 show the following: (i) When the expected solar generation was about 50% of the nominal capacity during all the periods of study, the total net savings with respect to the benchmark cases were US$/year 298,548.13 and US$/year 319,469.84 for the IEEE 33-bus and IEEE 69-bus systems. These values imply that in the worst possible operative scenario, the total investment and operating costs for PV sources are still recovered. (ii) As the availability of PV generation increases, the expected net savings increase, as these are a function of the reduction in the power generation in the slack source, i.e., the massive injection of power with renewable sources. However, realistic net saving values can be contained between 70% and 90% of PV generation, as these margins contain days with maximum generation and days with minimum values (e.g., 50% or lower).

Table 7. Effect of the solar generation availability on the total expected reduction in the annual operative costs.

PV (%)	A_{cost} (US$/year)	Net Savings (US$/year)	PV (%)	A_{cost} (US$/year)	Net Savings (US$/year)
50	3,401,907.26	298,548.13	50	3,558,730.09	319,469.84
60	3,257,488.59	442,966.79	60	3,407,395.45	470,804.47
70	3,115,174.01	585,281.37	70	3,258,562.51	619,637.42
80	2,974,867.30	725,588.09	80	3,112,096.01	766,103.92
90	2,836,480.36	863,975.03	90	2,967,873.44	910,326.49
100	2,699,932.29	1,000,523.09	100	2,825,783.33	1,052,416.60

6. Conclusions and Future Work

In this study, the problem of the optimal placement and sizing of renewable generators in radial grid-connected distribution networks was studied through the application of the DCCBGA using a master–slave optimization strategy. In the master optimization stage, the DCCBGA defines the optimal locations and sizes of the PV generators; and the slave stage, through the application of the successive approximation power flow method, determines the fitness function value. The objective of the studied problem corresponds to the simultaneous minimization of the energy purchasing costs in the substation bus, and the investment and operating costs of the PV generators installed.

The numerical results for the IEEE 33-bus and IEEE 69-bus systems were as follows:

- The reductions with respect to the benchmark cases reached by the DCCBGA were 27.04% and 27.14% for each test feeder, respectively. The BONMIN approach achieved a reduction of 26.99% in the IEEE 33-bus system and diverged for the IEEE 69-bus system.
- The percentage of solutions in the IEEE 33-bus system provided by the DCCBGA that improved upon the solution reported by the BONMIN solver was 44%, which demonstrated the efficiency of the proposed approach in finding alternative solutions. In the case of the IEEE 69-bus system, the solutions of the DCCBGA were compared with respect to the mean value and reported an efficiency of about 55%.
- Regarding the voltage profiles, in both test feeders, it was observed that during the period of maximum power injection (period of time 14), some nodes had higher values than the substation reference value, with magnitudes of 1.0215 and 1.0388 pu, respectively. Conversely, the minimum values were as expected during the period of time with maximum demand and zero PV injection (period of time 20) with values of 0.90378 and 0.90919 pu, respectively. These values confirmed that for all the time periods, the voltage profiles remained between the assigned bounds, i.e., $\pm 10\%$.

In the future, the following studies could be performed: (i) the simultaneous integration of photovoltaic and wind sources in grid-connected and non-interconnected areas considering the average generation costs with diesel sources; (ii) the application of new metaheuristic optimization techniques, such as the discrete-sine cosine algorithm, and the recently developed Newton metaheuristic algorithm, which was designed the studied problem; and (iii) inclusion of the MINLP formulation battery energy storage systems and their corresponding investment and operating costs.

Author Contributions: Conceptualization, methodology, software, and writing—review and editing, O.D.M., L.F.G.-N. and A.-J.P.-M. All authors have read and agreed to the published version of the manuscript.

Funding: This research was supported by Minciencias, Instituto Tecnológico Metropolitano, Universidad Nacional de Colombia and Universidad del Valle, under the research project "Estrategias de dimensionamiento, planeación y gestión inteligente de energía a partir de la integración y la optimización de las fuentes no convencionales, los sistemas de almacenamiento y cargas eléctricas, que permitan la generación de soluciones energéticas confiables para los territorios urbanos y rurales

de Colombia", which belongs to the research program "Estrategias para el desarrollo de sistemas energéticos sostenibles, confiables, eficientes y accesibles para el futuro de Colombia.

Conflicts of Interest: The authors declare no conflict of interest.

References

1. Tully, S. The Human Right to Access Electricity. *Electr. J.* **2006**, *19*, 30–39. doi:10.1016/j.tej.2006.02.003.
2. Lofquist, L. Is there a universal human right to electricity? *Int. J. Hum. Rights* **2019**, *24*, 711–723. doi:10.1080/13642987.2019.1671355.
3. Abdallah, L.; El-Shennawy, T. Reducing Carbon Dioxide Emissions from Electricity Sector Using Smart Electric Grid Applications. *J. Eng.* **2013**, *2013*, 845051. doi:10.1155/2013/845051.
4. Jursová, S.; Burchart-Korol, D.; Pustějovská, P.; Korol, J.; Blaut, A. Greenhouse Gas Emission Assessment from Electricity Production in the Czech Republic. *Environments* **2018**, *5*, 17. doi:10.3390/environments5010017.
5. Abdmouleh, Z.; Alammari, R.A.; Gastli, A. Review of policies encouraging renewable energy integration & best practices. *Renew. Sustain. Energy Rev.* **2015**, *45*, 249–262. doi:10.1016/j.rser.2015.01.035.
6. Braun, G.W. State policies for collaborative local renewable integration. *Electr. J.* **2020**, *33*, 106691. doi:10.1016/j.tej.2019.106691.
7. Muhammad, M.A.; Mokhlis, H.; Naidu, K.; Amin, A.; Franco, J.F.; Othman, M. Distribution Network Planning Enhancement via Network Reconfiguration and DG Integration Using Dataset Approach and Water Cycle Algorithm. *J. Mod. Power Syst. Clean Energy* **2020**, *8*, 86–93. doi:10.35833/mpce.2018.000503.
8. Hernandez, J.A.; Arredondo, C.A.; Rodriguez, D.J. Analysis of the law for the integration of non-conventional renewable energy sources (law 1715 of 2014) and its complementary decrees in Colombia. In Proceedings of the 2019 IEEE 46th Photovoltaic Specialists Conference (PVSC), Chicago, IL, USA, 16–21 June 2019. doi:10.1109/pvsc40753.2019.8981233.
9. Congreso de Colombia. *Ley No. 1715 del 13 de Mayo de 2014*; UPME: Medellin, Colombia, 2014; p. 26.
10. León-Vargas, F.; García-Jaramillo, M.; Krejci, E. Pre-feasibility of wind and solar systems for residential self-sufficiency in four urban locations of Colombia: Implication of new incentives included in Law 1715. *Renew. Energy* **2019**, *130*, 1082–1091. doi:10.1016/j.renene.2018.06.087.
11. López, A.R.; Krumm, A.; Schattenhofer, L.; Burandt, T.; Montoya, F.C.; Oberländer, N.; Oei, P.Y. Solar PV generation in Colombia—A qualitative and quantitative approach to analyze the potential of solar energy market. *Renew. Energy* **2020**, *148*, 1266–1279. doi:10.1016/j.renene.2019.10.066.
12. IPSE. *Boletín de Datos IPSE Septiembre 2021*; IPSE: Bogota, Colombia, 2021.
13. Delgado, R.; Wild, T.B.; Arguello, R.; Clarke, L.; Romero, G. Options for Colombia's mid-century deep decarbonization strategy. *Energy Strategy Rev.* **2020**, *32*, 100525. doi:10.1016/j.esr.2020.100525.
14. Colmenares-Quintero, R.F.; Maestre-Gongora, G.P.; Pacheco-Moreno, L.J.; Rojas, N.; Stansfield, K.E.; Colmenares-Quintero, J.C. Analysis of the energy service in non-interconnected zones of Colombia using business intelligence. *Cogent Eng.* **2021**, *8*, 1907970. doi:10.1080/23311916.2021.1907970.
15. Paz-Rodríguez, A.; Castro-Ordoñez, J.F.; Montoya, O.D.; Giral-Ramírez, D.A. Optimal Integration of Photovoltaic Sources in Distribution Networks for Daily Energy Losses Minimization Using the Vortex Search Algorithm. *Appl. Sci.* **2021**, *11*, 4418. doi:10.3390/app11104418.
16. Valencia, A.; Hincapie, R.A.; Gallego, R.A. Optimal location, selection, and operation of battery energy storage systems and renewable distributed generation in medium–low voltage distribution networks. *J. Energy Storage* **2021**, *34*, 102158. doi:10.1016/j.est.2020.102158.
17. Grisales-Noreña, L.; Montoya, D.G.; Ramos-Paja, C. Optimal Sizing and Location of Distributed Generators Based on PBIL and PSO Techniques. *Energies* **2018**, *11*, 1018. doi:10.3390/en11041018.
18. Helmi, A.M.; Carli, R.; Dotoli, M.; Ramadan, H.S. Efficient and Sustainable Reconfiguration of Distribution Networks via Metaheuristic Optimization. *IEEE Trans. Autom. Sci. Eng.* **2021**, early access. doi:10.1109/tase.2021.3072862.
19. Castiblanco-Pérez, C.M.; Toro-Rodríguez, D.E.; Montoya, O.D.; Giral-Ramírez, D.A. Optimal Placement and Sizing of D-STATCOM in Radial and Meshed Distribution Networks Using a Discrete-Continuous Version of the Genetic Algorithm. *Electronics* **2021**, *10*, 1452. doi:10.3390/electronics10121452.
20. Bhumkittipich, K.; Phuangpornpitak, W. Optimal Placement and Sizing of Distributed Generation for Power Loss Reduction Using Particle Swarm Optimization. *Energy Procedia* **2013**, *34*, 307–317. doi:10.1016/j.egypro.2013.06.759.
21. Ayodele, T.R.; Ogunjuyigbe, A.S.O.; Akinola, O.O. Optimal Location, Sizing, and Appropriate Technology Selection of Distributed Generators for Minimizing Power Loss Using Genetic Algorithm. *J. Renew. Energy* **2015**, *2015*, 832917. doi:10.1155/2015/832917.
22. Montoya, O.D.; Molina-Cabrera, A.; Chamorro, H.R.; Alvarado-Barrios, L.; Rivas-Trujillo, E. A Hybrid Approach Based on SOCP and the Discrete Version of the SCA for Optimal Placement and Sizing DGs in AC Distribution Networks. *Electronics* **2020**, *10*, 26. doi:10.3390/electronics10010026.
23. Sultana, S.; Roy, P.K. Krill herd algorithm for optimal location of distributed generator in radial distribution system. *Appl. Soft Comput.* **2016**, *40*, 391–404. doi:10.1016/j.asoc.2015.11.036.
24. Kaur, S.; Kumbhar, G.; Sharma, J. A MINLP technique for optimal placement of multiple DG units in distribution systems. *Int. J. Electr. Power Energy Syst.* **2014**, *63*, 609–617. doi:10.1016/j.ijepes.2014.06.023.
25. Montoya, O.D.; Gil-González, W.; Grisales-Noreña, L. An exact MINLP model for optimal location and sizing of DGs in distribution networks: A general algebraic modeling system approach. *Ain Shams Eng. J.* **2020**, *11*, 409–418. doi:10.1016/j.asej.2019.08.011.

26. Gil-González, W.; Montoya, O.D.; Grisales-Noreña, L.F.; Perea-Moreno, A.J.; Hernandez-Escobedo, Q. Optimal Placement and Sizing of Wind Generators in AC Grids Considering Reactive Power Capability and Wind Speed Curves. *Sustainability* **2020**, *12*, 2983. doi:10.3390/su12072983.
27. Buitrago-Velandia, A.F.; Montoya, O.D.; Gil-González, W. Dynamic Reactive Power Compensation in Power Systems through the Optimal Siting and Sizing of Photovoltaic Sources. *Resources* **2021**, *10*, 47. doi:10.3390/resources10050047.
28. Molina, A.; Montoya, O.D.; Gil-González, W. Exact minimization of the energy losses and the CO2 emissions in isolated DC distribution networks using PV sources. *DYNA* **2021**, *88*, 178–184. doi:10.15446/dyna.v88n217.93099.
29. Barbato, A.; Capone, A. Optimization Models and Methods for Demand-Side Management of Residential Users: A Survey. *Energies* **2014**, *7*, 5787–5824. doi:10.3390/en7095787.
30. Carli, R.; Dotoli, M. Energy scheduling of a smart home under nonlinear pricing. In Proceedings of the 53rd IEEE Conference on Decision and Control, Los Angeles, CA, USA, 15–17 December 2014. doi:10.1109/cdc.2014.7040273.
31. Bernal-Romero, D.L.; Montoya, O.D.; Arias-Londoño, A. Solution of the Optimal Reactive Power Flow Problem Using a Discrete-Continuous CBGA Implemented in the DigSILENT Programming Language. *Computers* **2021**, *10*, 151. doi:10.3390/computers10110151.
32. Chen, X.; Li, Z.; Wan, W.; Zhu, L.; Shao, Z. A master–slave solving method with adaptive model reformulation technique for water network synthesis using MINLP. *Sep. Purif. Technol.* **2012**, *98*, 516–530. doi:10.1016/j.seppur.2012.06.039.
33. McCall, J. Genetic algorithms for modelling and optimisation. *J. Comput. Appl. Math.* **2005**, *184*, 205–222. doi:10.1016/j.cam.2004.07.034.
34. Montoya, O.D.; Gil-González, W.; Orozco-Henao, C. Vortex search and Chu-Beasley genetic algorithms for optimal location and sizing of distributed generators in distribution networks: A novel hybrid approach. *Eng. Sci. Technol. Int. J.* **2020**, *23*, 1351–1363. doi:10.1016/j.jestch.2020.08.002.
35. Montoya, O.D.; Gil-González, W. On the numerical analysis based on successive approximations for power flow problems in AC distribution systems. *Electr. Power Syst. Res.* **2020**, *187*, 106454. doi:10.1016/j.epsr.2020.106454.
36. Shen, T.; Li, Y.; Xiang, J. A Graph-Based Power Flow Method for Balanced Distribution Systems. *Energies* **2018**, *11*, 511. doi:10.3390/en11030511.
37. Grisales-Noreña, L.F.; Montoya, O.D.; Ramos-Paja, C.A. An energy management system for optimal operation of BSS in DC distributed generation environments based on a parallel PSO algorithm. *J. Energy Storage* **2020**, *29*, 101488.
38. Wang, P.; Wang, W.; Xu, D. Optimal Sizing of Distributed Generations in DC Microgrids With Comprehensive Consideration of System Operation Modes and Operation Targets. *IEEE Access* **2018**, *6*, 31129–31140. doi:10.1109/access.2018.2842119.
39. Wang, Q.; Chang, P.; Bai, R.; Liu, W.; Dai, J.; Tang, Y. Mitigation Strategy for Duck Curve in High Photovoltaic Penetration Power System Using Concentrating Solar Power Station. *Energies* **2019**, *12*, 3521. doi:10.3390/en12183521.